Thermography based Breast Cancer Analysis: A Review

A. Arul Edwin Raj[1], Dr.T.Jaya[2], Dr.M Sundaram[3]

Associate Professor, ECE Department, Bethlahem Institute of Engineering, Karngal, Tamilnadu[1]

Professor, ECE Department, C.S.I Institute Of Technology, Thovalai, Tamilnadu[2]

Professor, ECE Department V.P.M.M. Engineering College for Women, Krishnankovil, Tamilnadu[3]

Abstract: Infrared thermography is an alternate to the thermometer to measure body temperature. Infrared (IR) camera can map the body temperature into intractable images. This paper provides a survey on the contribution of thermal images to analyze the breast cancer. The features are extracted from the mapped thermogram images for further image processing. This survey mainly concentrates on the comparison of statistical and texture features of normal and abnormal IR breast images, various types of segmentation and Region of Interest (ROI) extraction, modern IR camera specifications and various classification techniques to early detect the abnormality in the breast using thermal images obtained from the database.

Keywords: Spatial Features, IRT, DWT, Thermogram, SVM.

1 INTRODUCTION

Breast tumor is second common decease leads death for women after lung cancer [1]. Early Detection of breast cancer increases the possibilities of a patient's survival. Basically, the human body, health condition can be identified by abnormal temperature (>98.60 F). The normal temperature of the human body is $\approx 37^0$C. Any object that has above -273^0 K emit infrared wave from its surface [2,12]. So the human body emits infrared electromagnetic radiation. Thermography camera is sensitive to this kind of radiation, which captures the thermal variation of breast surface. Use of thermography to acquire the temperature of the human body is based on the metabolic activity and vascular circulation in both pre-cancerous tissue and area surrounding a developing breast cancer. The abnormal area in the breast emits temperature higher than normal breast tissue. Stefan-Boltzmann- law [3] described the relation between energy radiated from an object and its temperature. Stefan-Boltzmann- law states that "The total intensity radiated over all wavelengths increases as the temperature increases".
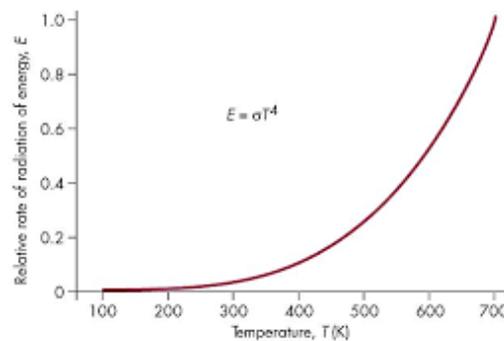

Fig.1.1 Stefan-Boltzmann- law

$$E = \sigma T^2 \qquad (1.1)$$

Where

E - Energy per unit area emitted by the body

T - Surface temperature of the body (in ^{0}K)

σ - the Stefan-Boltzmann constant

   - 5.67×10^{-8} Wm^{-2}K^{-4}

For real surfaces the Stefan Boltzman's law is modified to the following form

$$E = \varepsilon \, \sigma T^2 \qquad (1.2)$$

Where

ε – Emissivity of the emitting surface at a fixed wavelength and absolute temperature T.

2. INFRARED IMAGE

Thermal camera converts this energy into corresponding gray values of the corresponding point of the thermal image, that image has the minimum resolution of 320 X 320 pixels.
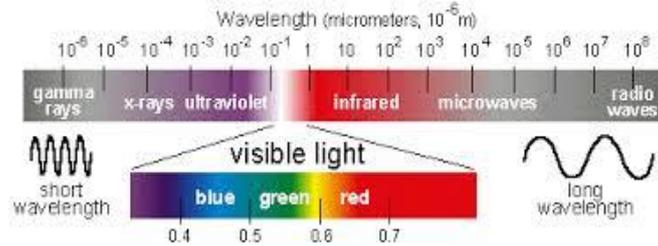

Fig 2.1 Electromagnetic Wave Spectrum

Figure 2 shows infrared wave below the red wave in the wave spectrum [23] so it is named as an infrared wave. Its wavelength is 0.75-1000 μm. It is further divided into three small groups near infrared (0.76 – 1.5μm), medium infrared (1.5 – 5.6μm) and far infrared (15μm - 1 mm). Hardy, in 1934 explained the physiological role of infrared emission from human bodies and proposed that human skin can be considered as a black body radiator. Planks Law state that blackboard is considered as a hypothetical object that absorbs all incident radiation and radiates a continuous spectrum. Medical thermography can be subdivided into four principal categories [5] depends on temperature sensing methodology 1. Electrical contact thermography 2. Cutaneous temperature discrimination 3. Liquid crystal thermography 4. Infrared Thermography (IRT). In electrical contact thermography, transducers made physical contact to measure surface temperature in the form of electrical current this current is mapped into the thermal image. In cutaneous temperature discrimination cutaneous receptors are the types of sensory receptor are used to response the light. Liquid crystal thermography, thermochromic cholesteric liquid crystal arranged in several layers it made good contact with the curved body surface. It changes its color due to changes in body temperature and gives the resultant pattern. In IRT thermal radiation emitted by the human body is detected by thermal camera as an image. Emissivity of human skin is reported to be almost constant and its value is 0.98 ± 0.01 for wavelength 2-14 μm. The surface curvature may cause changes in the emissivity. The emissivity [2] of a surface at a wavelength λ and viewing angle β is given as follows

$$\sum_{\Phi\lambda} = 1 - \left(\frac{1}{2}\left(\frac{\beta - cos\Phi}{\beta + cos\Phi}\right)^2\right)\left(1 + \left(\frac{\beta cos\Phi - sin^2\Phi}{\beta cos\Phi + sin^2\Phi}\right)^2\right) \qquad (2.1)$$

Where

$\beta - (n_\lambda{}^2 sin2\ \Phi\ )^{\frac{1}{2}}$

n_λ - Refractive index of the material

Φ – Viewing angle

3. EMISSIVITY

For a perfect blackbody emissivity is unity, but for real material's emissivity is always less than unity. The emissivity of different human tissues at infrared wavelengths [2] is tabulated below. Emissivity describes how to quantify the efficiency of a surface for radiating energy in a defined waveband and at a given temperature. Reality says any surface above absolute zero will always radiate some energy (more than 0%), and no surface can radiate perfectly (100%). Emissivity varies with surface condition, viewing angle, temperature, and spectral wavelength. Most nonmetallic materials are efficient radiators of energy. Human skin is close to a perfect radiator with an emissivity of 0.98.

Table 3.1: The emissivity of different human tissues at infrared wavelengths.

Tissue	Emissivity
Black skin (3–12 μm)	0.98 ± 0.01
White skin (3–14 μm)	0.97 ± 0.02
Burnt skin (3–14 μm)	0.97 ± 0.02
Epicardium (fresh: 0.5 h)	0.85
3 μm Epicardium (fresh: 0.5 h)	0.86
5 μm Epicardium	0.99
(9 days at 20^{0}C) Pericardium (3 μm)	0.88
Pericardium (5 μm)	0.94
Pericardium (9 μm)	0.95

Though the infrared emissions from human skin at 27^0 C lies within the wavelength range of 2–20 µm, it peaks around 10 µm. For medical applications in a very narrow wavelength band (8– 12 µm), termed as body infrared rays. With the advent of newer generations of detectors, Near Infrared (NIR) and Mid Infrared (MIR) regions are also used in medical thermography. The first modern infrared detector of lead-sulfide photo-detector was originally developed for military applications, around World War II. But later the technology was released for civilian uses and thereafter IRT has been used in medical sciences as well as in the field of non-destructive testing (NDT). In the field of NDT, the application of IRT is mainly in surface and sub-surface defect detection and online monitoring processes

Francisco et al [4] listed the values of the skin emissivity of the 40 participants as follows

Table 3.2: skin emissivity of the 40 participants [Francisco et al]

Subject	Emissivity	Subject	Emissivity
1	0.996	21	0.994
2	0.994	22	0.998
3	0.998	23	0.997
4	0.999	24	0.997
5	0.998	25	0.995
6	0.998	26	0.999
7	0.996	27	0.990
8	0.996	28	0.99
9	0.992	29	0.999
10	0.998	30	0.997
11	0.998	31	0.998
12	0.996	32	0.999
13	0.991	33	0.997
14	0.998	34	0.999
15	0.992	35	0.995
16	0.992	36	0.992
17	0.997	37	0.998
18	0.995	38	0.998
19	0.998	39	0.994
20	0.997	40	0.995

4.EXPERIMENTAL CONDITION FOR MEDICAL IRT

Human body thermal radiation depends on the experimental conditions standards such as experimental room, temperature control, subject information processing, imaging systems, image acquisition, image processing and result analysis.
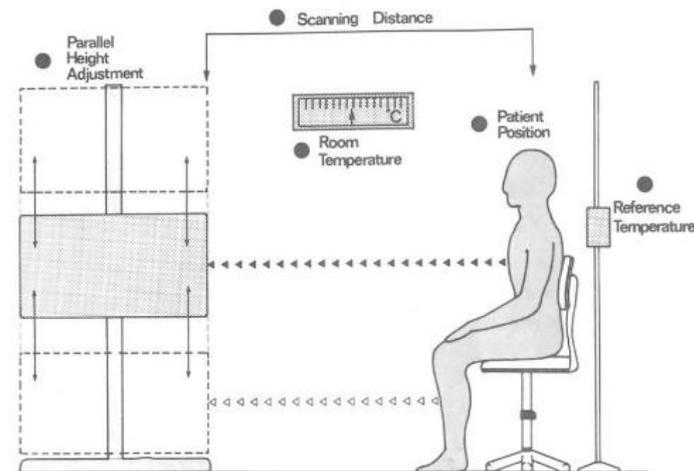

Fig 4.1 Thermal image experimental Setup

Table 4.1: Medical IRT experimental conditions standards

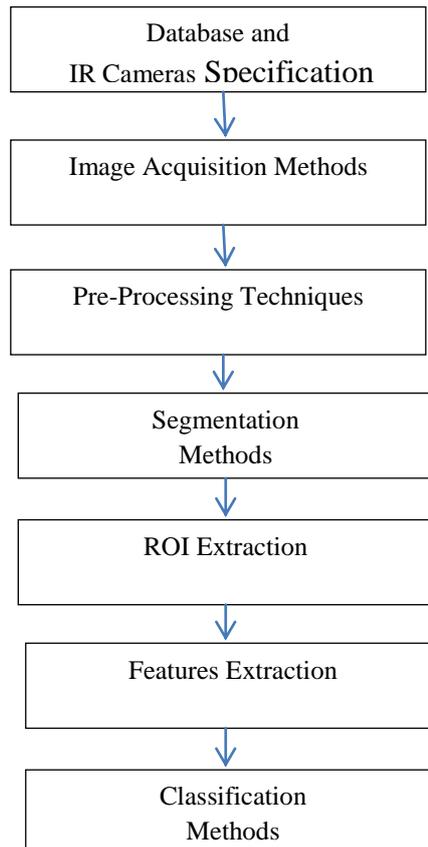| Parameter	How to set	Unit
Temperature	Temperature controls image quality. The user manual of FLIR provides the estimated temperature. Setup procedure: • Crumple up a large piece of aluminum foil • uncrumble it and put it in front of the sample facing the camera • Set the emissivity of 1 and measure the temperature. • Set this value as reflected temperature in the camera settings.	^{0}C
Emissivity	• Fix a piece of electrical tape of known emissivity onto the object • Set the emissivity mentioned in the camera manual, focus and write down the tape temperature • Make sure that the tape and the object are in the thermal equilibrium condition, point now to the sample surface and change the emissivity setting up of the camera shows the same temperature as the one previously recorded.	--
Humidity	A water molecule in the atmosphere change absorption of radiation emitted by the object. If the camera with humidity is it is possible to set the value at 50%.	--
Distance between object & camera	The distance between the object and the camera lens is doable easily by means of a ruler. Refer to the technical data sheet for the camera lens in order to respect the minimum focal length.	M
Atmospheric temperature	Camera working standard temperature is 20 to 400 °C. By using a thermometer, it can set directly.	^{0}C

Database and
IR Cameras Specification

↓

Image Acquisition Methods

↓

Pre-Processing Techniques

↓

Segmentation
Methods

↓

ROI Extraction

↓

Features Extraction

↓

Classification
Methods

Fig 4.2 Block diagram of survey flow

IJIREEICE

**International Journal of Innovative Research in
Electrical, Electronics, Instrumentation and Control Engineering**

ISO 3297:2007 Certified

Vol. 6, Issue 4, April 2018

4.1 Database and IR cameras

De Oliveria et al 2015 [7] collected breast thermal image from hospital Universitario Antonio Pedro which was approved by the ministry of health. Ng and Kee collected breast thermograms of 90 patients in Singapore General Hospital using thermal camera Avio TVS-2000. Mkll ST. Kontos [8] et al generated their own database of 63 patients using Meitherm MED 2000 thermal imaging system. It has two principle components the camera and the thermal evaluation software. It stores the data as a standard TIFF image file. Silva et al have developed their own Mamma Research with Infrared Image (DMR-IR) database, obtained from Antonio Pedro University Hospital patients by FLIR thermal camera, model SC620. Usha Rani Gogoi et al used existing DMR (Database for Mastology Research) Database is an online available database have used FLIR SC-620 Thermal Camera with a spatial resolution of 640 x 480 pixels. Swarthy et al obtained their database from the publicly available Iranian Thermography dataset. This image is acquired by using FLIR E30 Infrared Camera having 160X120 IR resolution.

4.2 Image Acquisition Methods

Sheeja v francis[1] et al have taken precool and post cool breast thermograms of 24 normal and 12 malignant patients as follows

- Patients were relaxed before thermogram taken, to stabilize body basal metabolic activities.
- Patient's one breast was on hold on a fixed temperature dark chamber to avoid interference.
- The thermal camera placed in the robotic arm, which fixed at a distance of 30–47 cm from the breast.
- The camera moved clockwise around the breast and imaged series of 12 images at the intervals of 30^0 angles.
- At first, 12 images of the left breast were taken in the chambers normal temperature called left precool series.
- Then the temperature of the chamber decreased by $2- 3^0$ centigrade and imaging was repeated as above and obtained set of 12 images called left post cool series.
- Then the robotic arm was moved and imaged the nipple region. This is named left frontal image.
- This procedure was repeated for the right breast, started with right frontal image; right precool series and right post cool series.

Kontos [8] et al followed the following procedure

- The room temperature was kept stable at approximately 22 ^{0}C, so that the patient was comfortable, and not perspiring nor shivering.
- The examination room had no windows and the vents were muffled, pointing away from the patient.
- The ceiling lights were fluorescent and invariably kept well away from the scanned area.
- Patients were asked to remove their clothes from their waist upwards and were left to equilibrate with ambient conditions for 10 - 15 min.
- Jewells and gowns were also removed.
- Then, they were instructed to sit in the middle of a rotation stool without a backrest, positioned at approximately 100 cm from the thermographic camera.
- Patients were asked to position their hands on the top of their head and remain still.
- Three images were obtained from each patient: one face (0^0) and one oblique on each side at 45^0 from the middle line for optimal exposure to all aspects of the breasts. The images were then appropriately labeled and stored as TIFF images.

Silva et al followed the following procedure

- Examination room windows and ventilations were blocked to control ambient temperature and airflows of the room
- A fluorescent lamp was positioned far from the patient.
- Number of persons in the examination room was limited
- Patients were asked to avoid smoke and drink caffeine or alcohol, for a certain time before the exam.
- Patients were asked to avoid applying a cosmetic on the exam day
- Inside the examination room the patient is asked to take off the cloths from the top of the body, laces, earrings and other accessories that may cause false readings.
- The patient was placed in front of the IR camera approximately one meter distance.
- Types of Image acquisition used are static and dynamic image acquisitions
- In static acquisitions the patient was instructed to take rest 10 and 15 minutes before examination, it changed small skin temperature during acquisition.
- In dynamic acquisition, patient was cooled by electric fan then temperature recovery was imaged.

Following steps were followed by E.Y and K. Ng [9]

- Patients were instructed to avoid sun bath on the area to be imaged at least 5 days before the examination,
- On the day of examination, Patients should avoid applying cream, lotion, deodorant and powder on the area going to take an image.
- If the imaging area to be shave it must be done at least 4 hours before the examination.
- No massage would be done from the previous day of examination.
- Avoid exercise at least 4 hours before the examination.
- Patients must consult the doctor to take the pain
   Medicine on the day of examination.
- Patients should avoid smoking and alcohol consumption.
- Patients should avoid taking excess meals, tea or coffee
- Patients should avoid tight wearing.
- Patients were relaxed about 15 minutes before examination for thermal stability.
- 3x4 meters, air–conditioned room was used as examination room
- During the examination Patients should be remain stationary.

Tiago B. Borchartt [10] et al followed the below steps

- Temperature controlled room (20–22°C) was used for examination.
- Humidity of the room was maintained at 60 %.
- The patient was relaxed about 15 minutes before examination for thermal stability.
- Patients were instructed to wear loose gown with proper air flow.
- Author mentioned recommended period for examination as between fifth and twelfth day after the menstrual cycle.

4.3 Preprocessing, Segmentation and ROI Extraction Techniques

4.3.1 Pre- Processing:
   The preprocessing is a process of selectively removing the redundancy available in the captured images without affecting the quality of the image. This process involves the following steps.

4.3.2 Image Re-sizing
It is performed by the process of the interpolation to re-samples the image to determine values between defined pixels [10]. So, resultant image contains more or less number of pixels than that of the input image. If the resolution of the output image is improved, the intensity of new pixels is obtained through interpolation process.

4.3.3 Filtering
   Due to the shake and improper camera zooming, uncertainties may happen into the image like as random noise, partial volume effects and intensity non uniformity. This may cause information loss, Signal to Noise Ratio (SNR) gain and degradation of edges. Spatial filters are used to remove this effect. Basically filters are classified as linear and nonlinear filters. Filtering masks are used by linear spatial filters and they are low pass filter and high pass filter. Nonlinear spatial filters operates with a coefficient of neighborhoods pixels directly. They are Median filter, Max filter and Min filter.

4.3.4 Segmentation
   Image segmentation is dividing a digital image into multiple segments (sets of pixels, also known as super-pixels) using basic properties of features of image like intensity, edge or texture [10, 11]. The segmented image is more understandable and easier to analyze. Two types of segmentation depending on the type of input image samples are gray scale single image segmentation and Histogram based segmentation. As the name stated the gray scale single image segmentation uses only one image for segmentation and feature extraction. It is subdivided into Edge based segmentation methods, Region growing segmentation methods and Threshold based segmentation methods. In Histogram based segmentation method, segmentation is based on the histogram of the image. It represents the gray levels of all the pixels of an image. Segmentation can be done by histogram peaks and the valleys between the pixels. Histogram based segmentation techniques are manual segmentation, histogram peak technique, histogram valley, adaptive histogram technique and Triangle thresholding technique.

4.4 ROI Extraction
   A Region of Interest (ROI) is a portion of an image that wants to filter or perform some other operation on. ROI can extract by creating a binary mask, which is a binary image that is the same size as the image you want to process.

Survey of various pre-processing techniques, method of segmentation, and different ROI extraction process are given below.

If any errors in automatic segmentation the entire CAD results gives wrong output. Because of this complexity, many authors, not prefer it for breast thermograms. For this reason Milosevic et al manually extracted ROI from the original thermograms. But some researchers are working on automatic segmentation. Phani Teja et al [13] has considered the lower part of the patient's breast image as the shape of a parabola so hough transform was used. EDDIE Y. -K. NG et al [9] initially used traditional snake and gradient vector flow snake for segmentation. But the method was not correctly able to fix the boundaries of the images. Hence, they modified the snake algorithm. They obtained derivative of the image by Roberts cross-gradient operators. Then these gradient images were processed by median filtering and sharpen by high pass filters. Gerald Schafer et al [15] segmented left and right breasts manually by experts. Leonardo S. Motta et al [16] used automatic segmentation to extract a region of interest of breast thermogram images with the help of automatic threading, automatic boundary detection, mathematical morphology, curve extraction and interpolation. Hossein Ghayoumi Zadeh et al [17] used a parabolic hough transform for Region of Interest (ROI) segmentation. For this purpose edges was detected by a logarithmic method. Their initial results of the edge detection were contaminated with high rates of noise. To remove this noise a Gaussian filter is used prior to edge detection. Dinsha D [18] presented a paper on breast tumor segmentation and classification of breast thermogram images. Here preprocessed breast thermogram image is enhanced by Contrast Limited Adaptive Histogram Equalization (CLAHE) technique. Then these images are filtered followed by segmenting the region of interest using k means and fuzzy C means. Various features are extracted from the segmented images.

4.5 Features Extraction:

Following features[6] were extracted from the spatial domain and it can be used for further processing.

4.5.1 Mean:

The mean estimates the value in the image in which central clustering occurs. The mean can be calculated using the formula:

$$\mu = \frac{1}{MN}\sum_{i=1}^{M}\sum_{j=1}^{N} p(i,j) \qquad (4.1)$$

Where p (i, j) is the pixel value at point (i, j) of an image of size M x N.

4.5.2 Variance:

The pixel intensities vary depending on thermogram image characteristics. This variation can be used for classification of micro-classification which can be estimated as given below:

$$\sigma^2 = \sum_{i,j} \frac{(x(i,j)-\mu)^2}{N} \qquad (4.2)$$

4.5.3 Standard deviation:

The standard deviation, σ is the estimate of the mean square deviation of gray pixel value p (i, j) from its mean value. Standard deviations describe the dispersion within a local region. It is determined using the formula:

$$S = \sqrt{\sigma^2} \qquad (4.3)$$

4.5.4 Smoothness:

Relative smoothness, R is a measure of grey level contrast that can be used to establish descriptors of relative smoothness. The smoothness is determined using the formula:

$$R = 1\frac{R}{1+\sigma^2} \qquad (4.4)$$

Where, σ is the standard deviation of the image.

4.5.5 Energy:

Ability to detect and visualize micro-classification can be improved using energy vector computation. The energy of thermogram image is computed by squaring and summing the pixels in transformed image and is given by:

$$E = \sum_x \sum_y (x-y)^2 I(x,y) \qquad (4.5)$$

Where I is the intensity of pixel value at x, y.

4.5.6 Contrast:

Contrast features extracted are used in classification to locate the micro - classification. Contrast information is estimated as

$$C = \sum_x \sum_y (x-y)^2 \, I(x,y) \tag{4.6}$$

4.5.7 Entropy :

The statistical evaluation of randomness which characterizes the texture feature in thermogram image is said to be entropy and is given by:

$$E_n = -\sum_x \sum_y p(x,y)\log[p(x,y)] \tag{4.7}$$

Where

p is the probability of occurrence of a particular pixel value.

4.5.8 Homogeneity :

The closeness of the distribution of pixel elements of ROI in thermogram image is computed using homogeneity and is given as:

$$H = \sum_x \sum_y \frac{p(x,y)}{1+(x-y)^2} \tag{4.8}$$

4.5.9 Kurtosis:

Estimates kurtosis value can distingush between the benign and malignant micro-classification through peaks and flat probability distribution which is given by:

$$K = \sum_{i=1}^{N} \frac{(I_i(x,y)-M_k)^2}{(N-1)\sigma^4} \tag{4.9}$$

Where

I (x-y)   Intensity of pixels,
N   Number of samples in circle lines
σ Standard deviation
M_k Mean of sub-bands

4.5.10 Correlation:

Nearby pixels of thermogram image are highly correlated which helps in identifying the similar regions. Correlation is estimated as:

$$\text{Correlation} = \sum_{i,j} \frac{(i=\mu_i)(j=\mu_j)p(i,j)}{\sigma_i \sigma_j} \tag{4.10}$$

4.5.11 Skewness:

This parameter indicates the lack of symmetry in distribution of pixels. This estimation gives an idea about symmetry and lack of symmetry within ROI in thermogram image.

$$\text{Skewness} = \sum_{i=1}^{N} \frac{(I_i(x,y)-M_k)^3}{(N-!)\sigma^3} \tag{4.11}$$

4.6 Feature Extraction Example:

A database for the example is referred from saga et al [1].

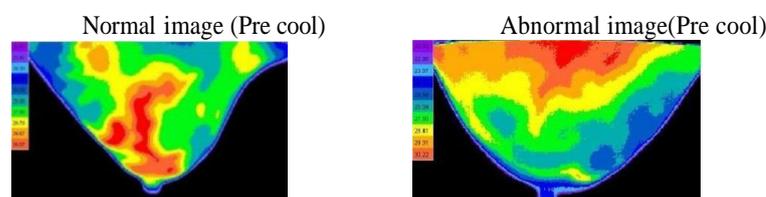Normal image (Pre cool)   Abnormal image(Pre cool)

Fig4.3 : Original image of normal and abnormal breast of pre-cooling

Contrast enhanced normal image(Pre cool)   Contrast enhanced abnormal image(Pre cool)

Fig 4.4 : Contrast enhanced normal and abnormal image of pre-cooling

Fig 4.5: Gray Scale of normal and abnormal image precooling

Thresholding normal Image (Pre cool)   Thresholding abnormal Image (Pre cool)
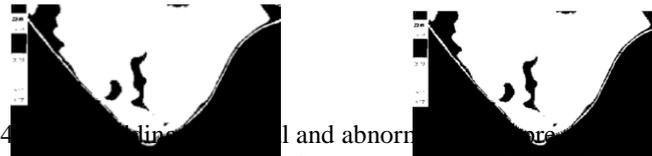
Fig 4. Thresholding normal and abnormal image pre

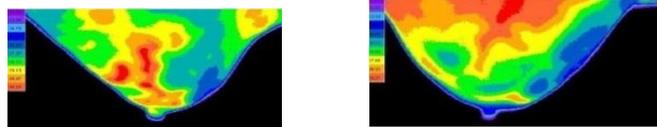Normal image (Post cool)   Abnormal image(Post cool)

Fig 4.7: Input image of normal and abnormal breast of post-cooling

Contrast enhanced normal image (Post cool)   Contrast enhanced abnormal image (Post cool)

Fig 4.8 : Contrast enhanced normal and abnormal image of pre-cooling

Fig 4.9 : Gray Scale of normal and abnormal image post cooling

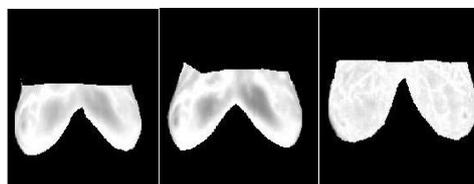Fig 4.10: Thersolding of normal and abnormal image post cooling

Fig 4.11: ROI of abnormal image of three patients

Table 4.2 : Statistical features of normal and abnormal image.

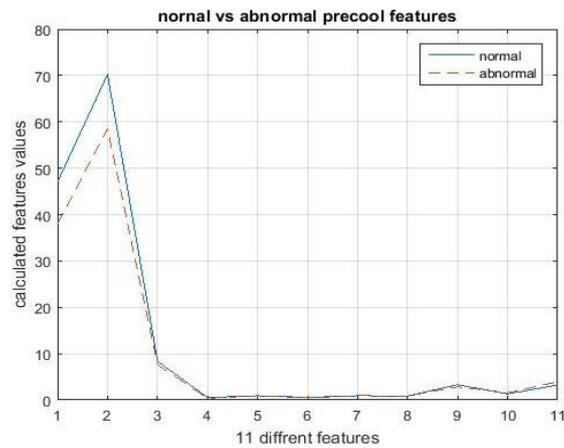| Features	Normal		abnormal	
	Pre-cool	Post-cool	Pre-cool	Post-cool
Mean	47.028	38.7018	37.9854	35.355
Varience	70.2607	58.2213	58.5326	55.1003
Standard	8.3822	7.6303	7.6507	7.423
Contrast	0.5463	0.2439	0.3677	0.2891
Correlation	0.948	0.9733	0.9576	0.9652
Energy	0.5146	0.5828	0.5856	0.6035
Homogeneity	0.9466	0.9536	0.9455	0.9495
Smoothness	0.8934	0.8841	0.8844	0.8813
Entrophy	3.3058	2.8359	2.8657	2.8359
skewness	1.3417	1.6313	1.5893	1.7161
kurtosis	3.2393	4.1097	3.9508	4.4308

Fig 4.12: Normal Vs Abnormal Pretcool Comparission
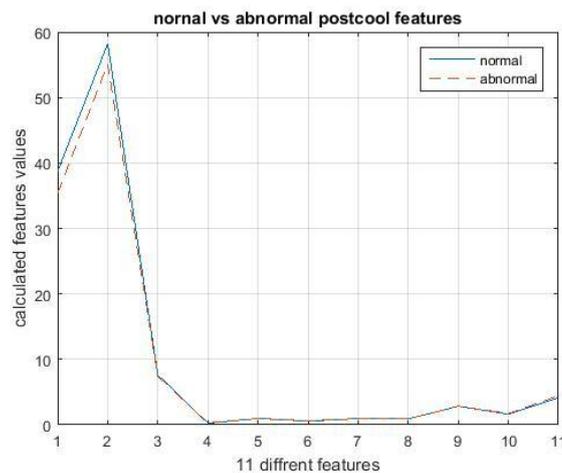
Fig 4.13: Normal Vs Abnormal Post Cool Comparison

features	normal1	normal2	normal3	abnormal1	abnormal2	abnormal3
Contrast	0.09681	0.097916	0.188723	0.113176	0.1823308	0.2089269
Correlation	0.065878	0.053614	0.110768	0.079735	0.1560352	0.0915779
Energy	0.859292	0.8642	0.802167	0.841944	0.8058964	0.788498
Homogeneity	0.963298	0.964031	0.94602	0.958965	0.9478971	0.9418289
Mean	0.001972	0.001864	0.002251	0.001919	0.003587	0.0036113
Stantard Deviation	0.063992	0.065071	0.082178	0.066792	0.0810406	0.0799917
Entropy	0.064018	3.285013	3.430739	3.176618	3.4343845	3.2937241
Variance	0.004061	0.004198	0.006742	0.004423	0.0065579	0.0063783
Smoothness	0.948139	0.943543	0.909047	0.942304	0.9405166	0.9403843
Kurtosis	7.426161	6.60871	7.342706	7.498896	8.2447941	8.372915
Skewnwss	0.354553	0.369806	0.623811	0.488093	0.7244895	0.6305528
IDM	0.626669	0.669739	0.378481	-0.78126	0.0716545	-0.9359379

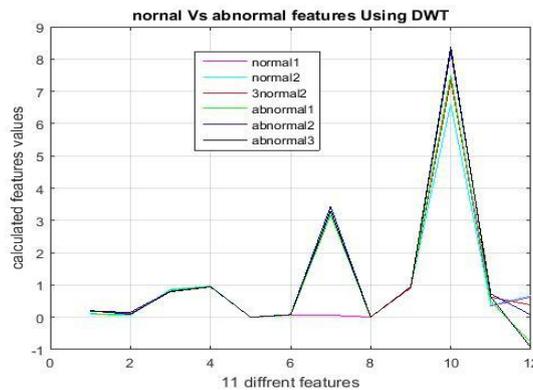Table 4.3: DWT features of normal and abnormal image.

Fig 4.14: Normal vs Abnormal feature comparison using DWT

5. CLASSIFIER PARAMETERS

1. Classification accuracy is dependent of the number of samples correctly classified.

$$A = \frac{TP + TN}{TP + TN + FA + FN}$$

2. Sensitivity is a proportion of positive cases that are well detected by the test

$$SE = \frac{TP}{TP+FP}$$

3. Specificity is a proportion of negative cases that are well detected by the test.

$$SP = \frac{TN}{TN+FP}$$

Where:

TP – True Positive
TN – True Negative
FP – False Positive
FN – False Negative

Table 5.1: Classification methods analysis

Classification method	Description	Characteristics
Artificial Neural network	Features were extracted using wavelet transforms(19). These features were used as an input of ANN. It used the additional nonlinear process to define the hidden layer.	The nonlinear Discriminant analysis approach was used. Accuracy depends upon the parameter selection of wavelet transform parameter, also structure of the network and number of inputs
Decision tree	Accuracy depends on training.. In the tree structure leaves is class mark and branches is a conjunction of components belongs to these classes. During the learning, subset is formed from the source set according to the parameters. This process is repeated until more separation is not useful [22].	It uses top down (hierarchical rule) algorithm to construct the tree. Distinctive algorithm is used to measure the best.
Support Vector Machine	It separates negative and positive examples using a hyper plane or hyper planes. SVM is a method of supervised learning it creates an input, output mapping with the help of labeled training data. It transforms input data into high-dimensional feature space 20]	The hyper plane selection and kernel parameter play the key role to accuracy and performance.
Fuzzy Measure	Fuzzy set elements have degrees of membership[21].. Fuzzy classification uses membership degrees and functions of fuzzy logic for classification. In Fuzzy classification, characteristics of an image are described by various stochastic associations. It provides different categories of stochastic characteristics in the similar form.	Threshold and fuzzy integral decide the accuracy and performance.

6. CONCLUSION

This survey covered comparison of statistical and texture features of normal and abnormal IR breast images, various types of segmentation and Region Of Interest (ROI) extraction, modern IR camera specifications and various classification techniques to early detect the abnormality of breast thermal image. Also, compared the pre cool and post cool IR image features (both normal and abnormal). Because of poor notification in this comparison, survey extends to a DWT feature extraction method and noticed the reasonable variation in both normal and abnormal DWT feature comparison. So the conclusion of this survey is, DWT feature extraction method is a better option than the pre cool and post cool method for thermography based breast cancer analysis.

REFERENCES

[1] Sheeja V Francis a, M. Sasikala "Breast cancer detection in rotational thermography images using texture features" Infrared Physics & Technology 67 (2014) pp. 490–496.
[2] B.B. Lahiri, S. Bagavathiappan "Medical applications of infrared thermography: A review" Infrared Physics & Technology 55 (2012) pp.221–235.
[3] www.britannica.com/science/Stefan-Boltzmann-law.
[4] Francisco J. Sanchez-Marin, Sergio Calixto-Carrera "Novel approach to assess the emissivity of the human skin" Journal of Biomedical Optics vol.14(2), pp. 024006-1 - 024006-6 March/April 2009.
[5] Ruben Usamentiaga ,Pablo Venegas "Infrared Thermography for Temperature Measurement and Non-Destructive Testing" Sensors 2014, pp.12305-12348.
[6] Marina Milosevic, Dragan Jankovic "Thermography based breast cancer detection using texture features and minimum variance quantization" EXCLI Journal 2014; vol.13 pp.1204-1215
[7] De Oliveira A.Conci, Maria G.perez "Segmentation of infrared images: a new technology for early detection of breast diseases" Industrial Technology (ICIT), IEEE International Conference 2015; pp.1765-1771.
[8] M. Kontos a , R. Wilson b , I. Fentiman a "Digital infrared thermal imaging (DITI) of breast lesions: sensitivity and specificity of detection of primary breast cancers "Clinical Radiology vol66 (2011) pp.536-539.

[9]   E.Y and K. Ng "A review of thermography as promising non-invasive detection modality for breast tumor" International Journal of Thermal Sciences vol. 48 (2009) pp.849–859.

[10]   Tiago B. Borchartt "Breast thermography from an image processing viewpoint: A survey" Signal Processing vol.93 (2013) pp.2785–2803.

[11]   U. Rajendra Acharya , E. Y. K. Ng "Thermography Based Breast Cancer Detection Using Texture Features and Support Vector Machine" Springer Science and Business Media vol.36 pp.1503–1510.

[12]   E. Y. K. Ng a , Y. Chen "Computerized breast thermography: study of image segmentation and temperature cyclic variations" Journal of Medical Engineering & Technology, Volume 25,(2001) , pp. 12 – 16.

[13]   Phani Teja Kuruganti, Hairong Qi "Asymmetry Analysis in Breast Cancer Detection Using Thermal Infrared Images" EMBSiBMES Conference Houston, USA (2002) pp.1155-1156.

[14]   Subbhuraam Vinitha Sree, Eddie Yin-Kwee Ng "Breast imaging: A survey" World J Clin Oncol. 2011 pp.: 171–178.

[15]   G. Schafer, M. Zavisek, and T. Nakashima, "Thermography based breast cancer analysis using statistical features and fuzzy classification," Journal on Pattern Recognition(Jun. 2009), vol. 42, pp. 1133- 1137.

[16]   L. S. Motta, A. Conci1, R. C. F. Lima, and E. M. Diniz, "Automatic segmentation on thermograms in order to aid diagnosis and 2D modeling," in Proc. Anais CSBC, Belo Horizonte, Minas Gerais, Brazil, 2010. pp.1611 – 1619.

[17]   Hossein Ghayoumi Zadeh, Javad Haddadnia "Segmenting breast cancerous regions in thermal images using fuzzy active contours" EXCLI Journal Vols 15; 2016

[18]   D. Dinsha, "Breast tumor segmentation and classification using SVM and Bayesian from thermogram images," Unique Journal of Engineering and Advanced Sciences, vol. 2, pp. 147-151, 2014.

[19]   E. Y. K. Ng, L. N. Ung "Statistical analysis of healthy and malignant breast thermography" Journal of Medical Engineering & Technology, Volume 25,pp. 253 – 263.

[20]   U. Rajendra Acharya , E. Y. K. Ng "Thermography Based Breast Cancer Detection Using Texture Features and Support Vector Machine" Springer Science and Business Media(2012), vol.36, pp. 1503–1510.

[21]   Gerald Schaefer , Michal Zavisek "Thermography based breast cancer analysis using statistical features and fuzzy classification" Loughborough University's Institutional Repository(2009) vol. 42 (6), pp. 1133 - 1137.

[22]   Hanif Yaghoobi, Alireza Ghahramani "Breast Cancer Diagnosis Using, Gray-Level Co-Occurrence, Decision Tree Classification and Evoltionary Feature Selection" International Conference on knowledge- Based Engineering and Innavation(2015) pp.317-328.

[23]   https://en.wikipedia.org/wiki/Infrared